

A Novel Active Snubber for High-Power Boost Converters

Milan M. Jovanović, *Senior Member, IEEE*, and Yungtaek Jang, *Member, IEEE*

Abstract—A technique which improves the performance of the boost converter by reducing the reverse-recovery-related losses in the boost switch and rectifier with an active snubber that is implemented with a minimum number of components is presented. This minimum-component-count snubber consists of a snubber inductor, an auxiliary switch, and a rectifier. The proposed technique reduces the reverse-recovery-related losses by controlling the turn-off di/dt rate of the rectifier current with the snubber inductor connected in series with the boost switch and rectifier. The voltage and current stresses of the components in the proposed active-snubber boost converter are similar to those in its conventional “hard-switched” counterpart.

Index Terms—Active snubber, boost converter, power factor correction, reverse recovery loss, zero voltage switching.

I. INTRODUCTION

AT HIGHER power levels, the continuous-conduction-mode boost converter is the preferred topology for implementing a front end with active input-current shaping. As a result, in recent years, significant efforts have been made on improving the performance of high-power boost converters. The majority of these development efforts have been focused on reducing the adverse effects of the reverse-recovery characteristic of the boost rectifier on the conversion efficiency and electromagnetic compatibility (EMC) [1].

Generally, the reduction of the reverse-recovery-related losses and EMC problems requires that the boost rectifier be “softly” switched off by controlling the turn-off rate of its current. For a majority of today’s rectifiers the optimal turn-off di/dt rate is below 100 A/ μ S.

So far, a number of soft-switched boost converters and their variations have been proposed [2]–[10]. All of them use additional components to form an active snubber [2]–[7], or a passive lossless snubber [8]–[10] circuit that controls the turn-off di/dt rate of the boost rectifier. Generally, the active-snubber approaches employ an auxiliary active switch with a few passive components such as inductors, capacitors, and rectifiers, whereas the passive-snubber approaches use only passive components.

The main feature of the active approaches introduced in [2]–[7] is that besides soft switching of the boost rectifier they also offer the zero-voltage switching (ZVS) of the boost switch. In addition, the approaches described in [4]–[7] offer soft switching of the auxiliary switch. Specifically, in the

active-snubber implementation in [4], the snubber switch turns off with zero-current switching (ZCS), whereas in the implementations in [5]–[7], it turns on with ZVS. In addition, all these active approaches exhibit voltage and current stresses on the semiconductor components which are similar to those in the boost circuit without a snubber. The major downside of the active snubber approaches is a relatively large component count, as well as the need for a driver for the snubber’s active switch. Moreover, the active snubbers introduced in [5]–[7] require a less-desirable, isolated (high-side) drive for the snubber switch.

Generally, the passive lossless snubbers are as effective as the active snubbers in reducing the reverse-recovery-related losses because they implement the soft switching of the boost rectifier in a similar way as the active snubbers. However, the passive snubbers do not offer ZVS of the boost switch. This does not have a significant detrimental effect on the conversion efficiency since the efficiency reduction because of the capacitive turn-on loss of the boost switch due to the absence of ZVS is typically less than 0.5%. The major drawback of the passive approaches is a significantly increased voltage and/or current stress on the semiconductor components [8]–[10]. This increased stress dictates the use of higher-rated and, usually, more expensive components. Additionally, some passive-snubber implementations require a relatively large number of passive components.

In this paper, a simple active-snubber implementation for the boost power stage is proposed. The snubber is implemented with only three components and it offers both the soft switching of the boost rectifier and the snubber switch. In addition, this minimum-component-count active snubber employs a direct (non-isolated) drive for the snubber switch, and operates with overlapping gate-drive signals of the boost and snubber switches, which enhances the robustness of the circuit. The voltage and current stresses of the components in this active-snubber boost converter are similar to those in its conventional “hard-switched” counterpart. Finally, it was verified experimentally on a 1-kW, universal-input boost power stage that the proposed active snubber is effective in extending the power range of the boost converter by reducing the reverse-recovery-related losses.

II. ANALYSIS OF OPERATION

The circuit diagram of the boost converter which employs the new technique for reverse-recovery-loss reduction is shown in Fig. 1. The circuit in Fig. 1 uses snubber inductor L_S connected in series with boost switch S and rectifier D to control the di/dt rate of the rectifier. The snubber action is controlled by auxiliary

Manuscript received February 2, 1999; revised July 22, 1999. Recommended by Associate Editor, J. Enslin.

The authors are with the Delta Products Corporation, Power Electronics Laboratory, Research Triangle Park, NC 27709 USA.

Publisher Item Identifier S 0885-8993(00)02343-7.

switch S_1 which is connected between the anode of boost rectifier D and the circuit ground. The function of snubber rectifier D_S is to clamp the voltage across main switch S to the output voltage after switch S is turned off.

To simplify the analysis of operation, it is assumed that the inductance of boost inductor L is large so that it can be represented by constant-current source I_{IN} , and that the output-ripple voltage is negligible so that the voltage across the output filter capacitor can be represented by constant-voltage source V_O . Also, it is assumed that in the on-state semiconductors exhibit zero resistance, i.e., they are short circuits. However, the output capacitance of the switches and the reverse-recovery charge of the rectifiers are not neglected in this analysis. The circuit diagram of the simplified converter, as well as the reference directions for currents and voltages are shown in Fig. 2.

To further facilitate the explanation of the operation, Fig. 3 shows topological stages of the circuit in Fig. 1 during a switching cycle, whereas Fig. 4 shows the power-stage key waveforms. As can be seen from the gate-drive timing diagrams for the boost and auxiliary switches in Fig. 4, the proposed circuit operates with an overlapping gate drive of the switches, i.e., both switches conduct simultaneously.

Before main switch S is turned on at $t = T_0$, the entire input current I_{IN} flows through snubber inductor L_S and boost rectifier D . At the same time, auxiliary switch S_1 is off blocking voltage V_O , whereas snubber rectifier D_S , ideally, carries no current.

After switch S is turned on at $t = T_0$, constant voltage V_O is applied across L_S , as shown in Fig. 3(a). As a result, inductor current i_{LS} and rectifier current i_D decreases linearly, whereas switch current i_S increases at the same rate. The rate of the rectifier current decrease is governed by

$$\frac{di_D}{dt} = -\frac{V_O}{L_S} \quad (1)$$

Since the rate of the boost rectifier current decrease is controlled by snubber inductance L_S , the rectifier's recovered charge and the associated losses can be reduced by a proper selection of the L_S inductance. Generally, a larger inductance, which gives a lower di_D/dt rate, results in a more efficient reduction of the reverse-recovery-associated losses [1].

At $t = T_1$, when i_{LS} and i_D decrease to zero, the entire input current I_{IN} flows through switch S , as shown in Fig. 4. Ideally, when i_D falls to zero at $t = T_1$, rectifier D should stop conducting. However, due to a residual stored charge, reverse-recovery current i_{RR} will flow through rectifier D , as shown in Fig. 3(b). After rectifier D recovers at $t = T_2$, the rectifier stops conducting, and output capacitance C_{OSS1} of switch S_1 starts discharging in a resonant fashion by current i_{LS} , as shown in Fig. 3(c). During this resonance, negative snubber-inductor current i_{LS} increases by the amount of $V_O/\sqrt{L_S/C_{OSS1}}$, as indicated in the i_{LS} waveform in Fig. 4. After C_{OSS1} is completely discharged at $t = T_3$, current i_{LS} which was flowing through C_{OSS1} continues to flow through antiparallel diode D_{AP1} of auxiliary switch S_1 , as indicated in Fig. 3(d).

Since at $t = T_4$ when auxiliary switch S_1 is closed its antiparallel diode D_{AP1} is conducting, auxiliary switch S_1 always

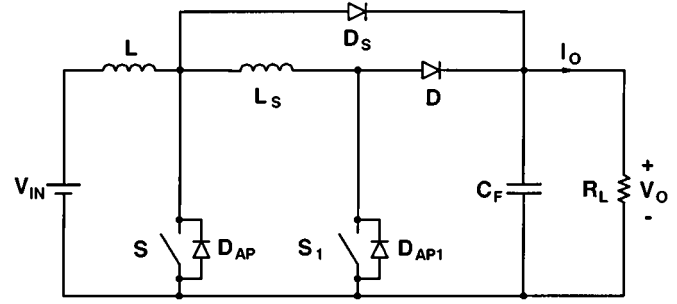


Fig. 1. Boost power stage with minimum-component-count active snubber.

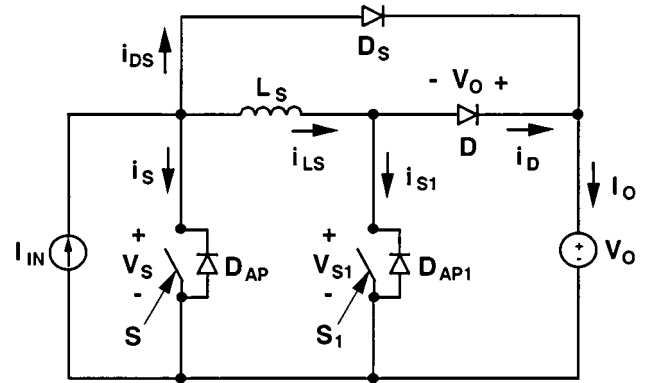


Fig. 2. Simplified circuit diagram of the proposed boost power stage showing reference directions of currents and voltages.

turns on under ZVS condition. After switch S_1 is turned on, current i_{LS} continues to flow through switch S_1 instead through its antiparallel diode D_{AP1} , as shown in Fig. 3(e).

After main switch S is turned off at $t = T_5$, switch current i_S is diverted from the switch to its output capacitance C_{OSS} , as shown in Fig. 3(f). As a result, voltage across switch S , v_S , increases. Since, typically, input current I_{IN} is much larger than $|i_{LS}| = |i_{RR} + V_O/\sqrt{L_S/C_{OSS1}}|$, the increase of v_S is essentially linear, as illustrated in Fig. 4. At the same time, i_{LS} starts to slowly increase from its initial negative value due to rising switch voltage v_S . When v_S reaches V_O at $t = T_6$, switch current i_S which was charging C_{OSS} is diverted to snubber rectifier D_S , as shown in Fig. 3(g). Since after D_S starts conducting at $t = T_6$, constant positive voltage V_O is applied across L_S , current i_{LS} continues to increase linearly, as shown in Fig. 4. At the same time, snubber-rectifier current i_{DS} decreases at the same rate because the sum of i_{LS} and i_{DS} is equal to the constant input current I_{IN} . When i_{DS} reaches zero at $t = T_7$, D_S turns off.

After D_S stops conducting at $t = T_7$ the circuit can have different modes of operation depending on the time that auxiliary switch S_1 is still kept on. For optimal performance, switch S_1 should be turned off immediately after i_{DS} reaches zero, as it will be discussed in the next section. When switch S_1 is turned off at $t = T_7$, inductor current $i_{LS} = I_{IN}$, which was flowing through switch S_1 , is diverted to output capacitance C_{OSS1} , as shown in Fig. 3(h). Because of a constant-current charging, v_{S1} increases linearly toward V_O , whereas v_D decreases linearly toward zero, as illustrated in Fig. 4. When, at $t = T_8$, v_{S1} reaches

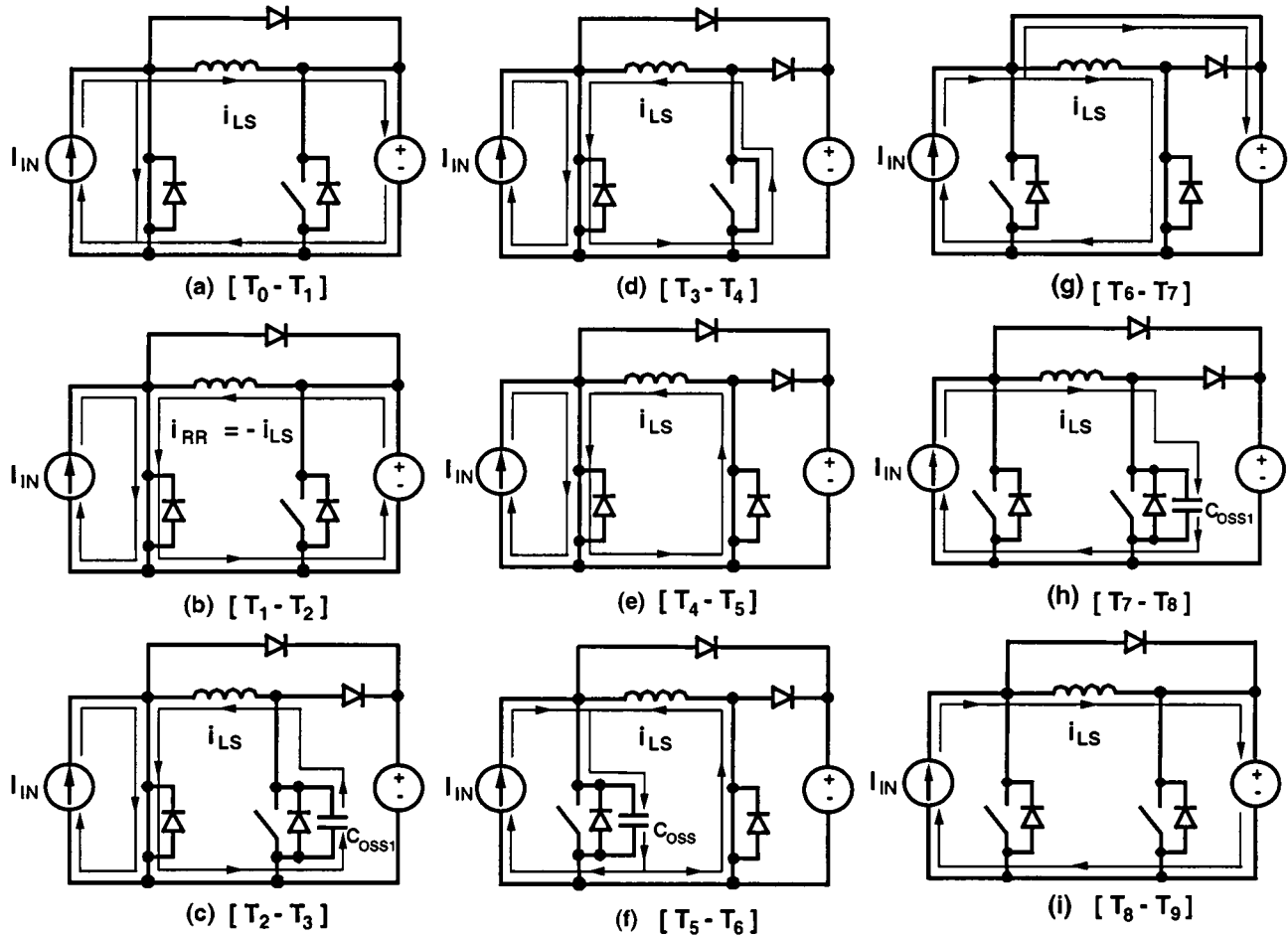


Fig. 3. Topological stages of the proposed boost power stage.

V_O , boost rectifier D becomes forward bias, and $i_{LS} = I_{IN}$ is commutated from C_{OSS1} to rectifier D , as shown in Fig. 3(i). I_{IN} continues to flow through D until a new switching cycle is initiated by turning on switch S at $t = T_9$.

III. DESIGN GUIDELINES

Generally, the design of the proposed boost converter with the active snubber follows the well-established design rules for the conventional boost power stage since for a properly designed converter with the active snubber the effect of the snubber circuit on the operation and conversion characteristic of the boost power stage is negligible. Specifically, if the commutation time of boost-inductor current I_{IN} from boost rectifier D to boost switch S , i.e., time interval $T_3 - T_0$ shown in Fig. 4, is short compared to a switching period, the snubber circuit has no significant effect on the operation of the boost power stage. Otherwise, the conversion-ratio of the boost power stage becomes strongly dependent on the load current, as described in [7].

To reduce the recovered charge of today's fast-recovery rectifiers, it is necessary to reduce their turn-off di/dt rate to approximately below $100 \text{ A}/\mu\text{S}$ [1]. Generally, reducing the di/dt rate much below $100 \text{ A}/\mu\text{S}$ does not decrease the recovered charge significantly. Therefore, to keep the di/dt rate below $100 \text{ A}/\mu\text{S}$

for a typical output voltage of $V_O = 400 \text{ V}$, the minimum required L_S is $400 \text{ V}/100 \text{ A}/\mu\text{s} = 4 \mu\text{H}$. In fact, for the optimal performance of the majority of today's fast-recovery rectifiers, a snubber inductance in the $4\text{-}\mu\text{H}$ to $6\text{-}\mu\text{H}$ range seems to be the best choice.

It should be noted that for snubber inductance L_S in the $4\text{-}\mu\text{H}$ to $6\text{-}\mu\text{H}$ range, the commutation time $T_3 - T_0$ of the boost current is extremely short. For example, for a 1-kW ($400 \text{ V}/2.5 \text{ A}$) boost power stage operating from an input voltage of $V_{IN} = 90 \text{ V}$, commutation time $T_3 - T_0 \sim T_1 - T_0 = I_{IN} L_S / V_O = I_O L_S / V_{IN} = (2.5 \text{ A})(4.7 \mu\text{H}) / (90 \text{ V}) = 0.13 \mu\text{s}$. This commutation time is approximately 77 times shorter than the switching period of $10 \mu\text{s}$ which corresponds to the 100 kHz switching frequency that is a reasonable choice at this power level.

Since the maximum current and maximum voltage of all semiconductors in the proposed circuit are limited to maximum (low-line) input current $I_{IN(\max)}$ and output voltage V_O , respectively, the current and voltage rating of the switches and rectifiers should be selected following the same derating rules as for the conventional boost converter. However, it should be noted that the rms current of auxiliary switch S_1 and snubber rectifier D_S are much lower than the rms current of boost switch S and rectifier D . As a result, the required power ratings of switch S_1 and rectifier D_S are lower than those of switch S and rectifier D .

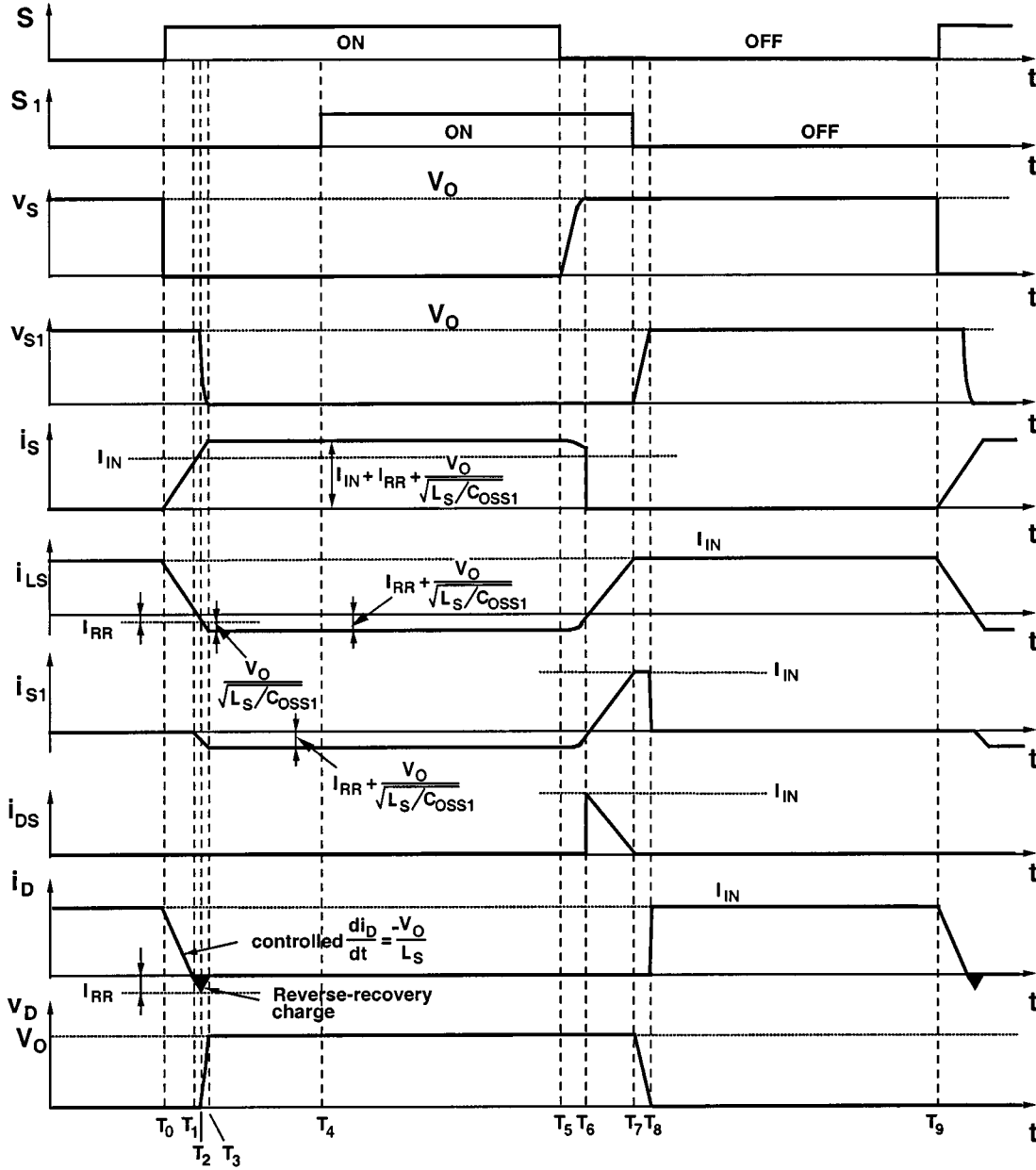


Fig. 4. Key waveforms of the proposed boost power stage.

To maximize the conversion efficiency, a proper timing of the auxiliary-switch gate drive is critical. Generally, to achieve zero-voltage switching, auxiliary switch S_1 should be turned on after main switch S is turned on and while its body diode D_{AP1} is conducting. Because of a long conduction interval of D_{AP1} , the turn-on timing of S_1 is not a problem. However, the turn-off timing of S_1 requires more attention. Namely, if auxiliary switch S_1 stays closed much longer after i_{DS} reaches zero at $t = T_7$, the output capacitance of switch S , C_{OSS} , the junction capacitance of snubber rectifier D_S , C_{JS} , and snubber inductor L_S will resonate. This resonance increases snubber inductor current i_{LS} above I_{IN} so that when S_1 is eventually turned off, snubber rectifier D_S ends up carrying the current in excess of I_{IN} that is created by the resonance, whereas rectifier D carries current I_{IN} . As a result, when boost switch S is turned on, snubber rectifier D_S introduces reverse-recovery

losses since the anode of D_S is directly connected to switch S . Because the current flowing through D_S is generally small, the reverse-recovery-related losses due to a “hard” turn-off of D_S are relatively small. Nevertheless, to maximize the efficiency this loss should be minimized. Therefore, for an optimally designed converter, the fixed time interval between the turn-off of main switch S and the turn-off of auxiliary switch S_1 should be adjusted so that at low line and full load switch S_1 is turned off at the moment current i_{DS} reaches zero. Although for such an adjustment of the gate-drive signals current i_{DS} is not zero at the moment S_1 is turned off at other line and load conditions, i_{DS} is still small enough so it does not introduce significant reverse-recovery related losses.

Finally, it should be also noted that the control of the proposed boost converter could be implemented in the same way as in its conventional “hard” switched counterpart as long as

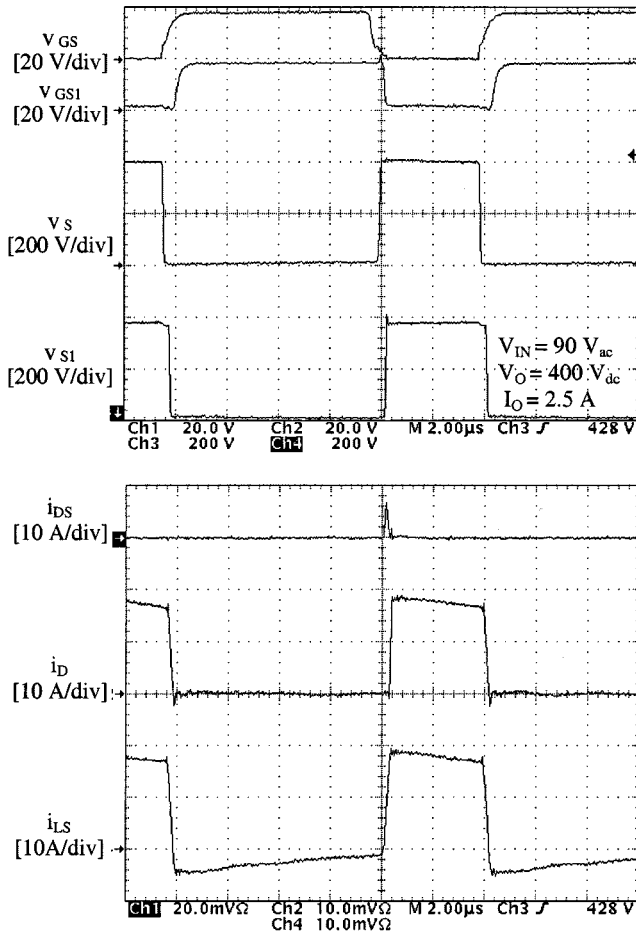


Fig. 5. Measured key waveforms of experimental converter at $P_O = 1$ kW and $V_{IN} = 90$ V_{ac}. Time base: 2 μ s/div.

an additional gate-driver circuit is provided. Specifically, in the input-current-shaping applications, the proposed converter can be implemented with any known control technique, such as average current, peak current, or hysteretic control.

IV. EXPERIMENTAL RESULTS

The performance of the boost converter with the proposed active snubber was evaluated on a 1-kW (400 V/2.5 A), universal-line-range (90–265 V_{ac}) power-factor-correction circuit operating at 80 kHz. For comparison purposes, the experimental circuit was implemented using both an IGBT and a MOSFET for main switch S . The other components in both experimental implementations were the same. The experimental circuit were implemented using the following components: boost switch S —IXGK50N60B (IGBT implementation), IXFK48N50 (MOSFET implementation); auxiliary switch S_1 —2SK2837 (MOSFET); boost rectifier D —two RHRP3060 connected in parallel; boost inductor $L = 0.8$ mH; snubber inductor $L_S = 4.7$ μ H; snubber rectifier D_S —RHRP3060, and bulk capacitor $C_F =$ two 470 μ F/450 V connected in parallel.

Boost inductor L was built using Magnetics toroidal core (Kool Mu 77439-A7, two cores in parallel) and 55 turns of AWG#14, whereas snubber inductor L_S was built with Magnetics toroidal core (Kool Mu 77932-A7) with 12 turns of

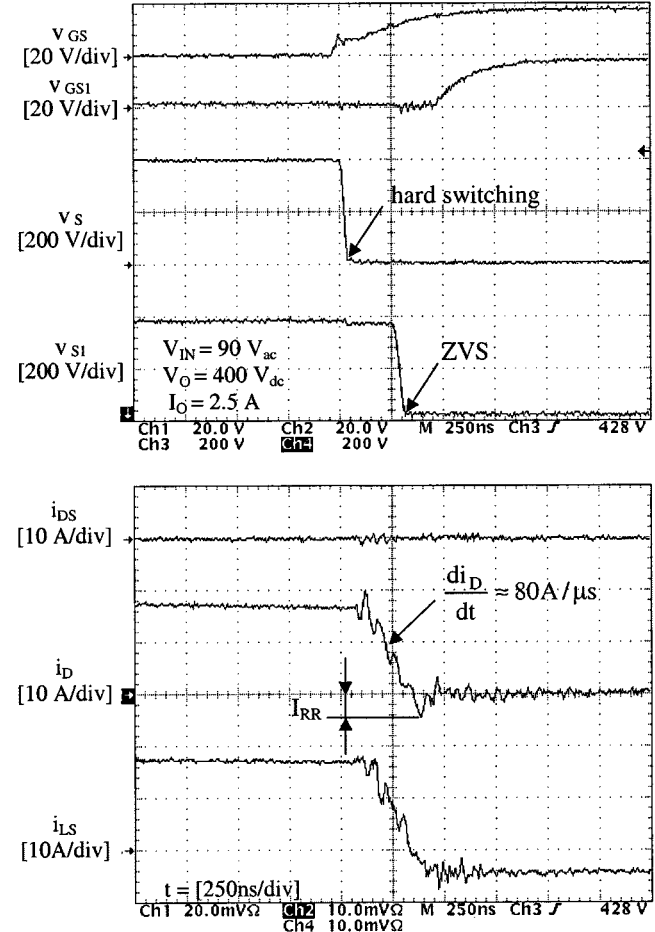


Fig. 6. Detailed view of key waveforms shown in Fig. 5 during turn-on transition. Time base: 250 ns/div.

AWG#14. With the selection of $L_S = 4.7$ μ H, the di/dt turn-off rate of the rectifier was limited to $di_D/dt = V_O/L_S = 80$ A/ μ s. The control circuit was implemented with the average-current PFC controller UC3854. The TC4420 and TSC428 drivers were used to generate the required gate-drive signals for the main and auxiliary switches, respectively.

Fig. 5 shows the oscillograms of key waveforms of the IGBT implementation of the experimental converter at the low line and full power. As can be seen comparing corresponding waveforms in Figs. 4 and Fig. 5, there is a good agreement between the experimental and theoretical waveforms. The more detailed oscillograms of the key waveforms in Fig. 5 around the turn-on and turn-off transition of the boost switch are shown in Figs. 6 and 7, respectively. As can be seen from Fig. 6, auxiliary switch S_1 is turned on with ZVS since its voltage V_{S1} falls to zero before gate-drive signal V_{GS1} becomes high. However, boost switch S is “hard” switched, i.e., S is turned on while voltage across it $v_S = V_O = 400$ V. Despite the “hard” switching of boost switch S , all waveforms are ringing free. Also, it should be noted that the boost-rectifier-current turn-off rate, which is controlled by L_S , is approximately $di_D/dt = 80$ A/ μ s, as indicated in Fig. 6. With this di_D/dt rate, peak reverse-recovery current I_{RR} is reduced to approximately 4 A, which corresponds to a recovered charge of approximately 100 nC. Finally, as shown in Fig. 7, the

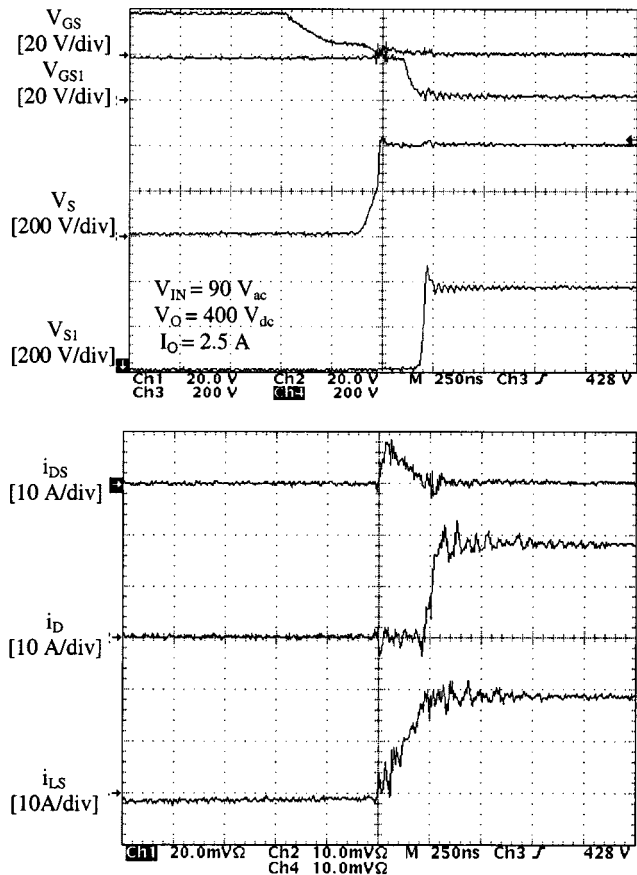


Fig. 7. Detailed view of key waveforms shown in Fig. 5 during turn-off transition. Time base: 250 ns/div.

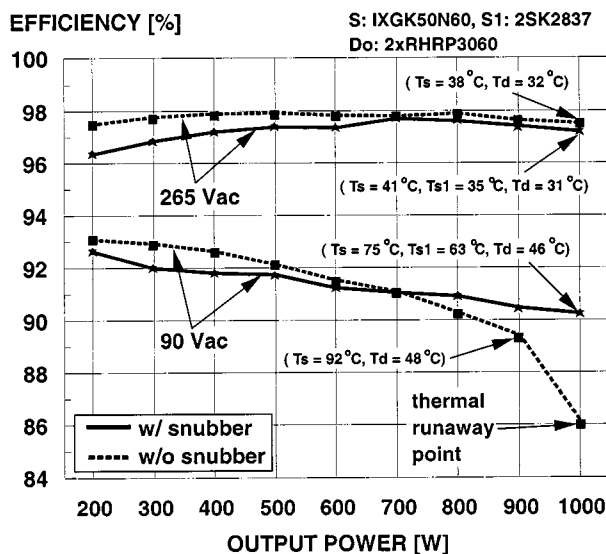


Fig. 8. Measured efficiency of 1-kW experimental circuit implemented with IGBT boost switch.

voltage across boost switch S is well clamped by D_S during the switch S turn-off.

Fig. 8 shows the measured efficiencies of the IGBT implementation of the experimental converter with and without the active snubber at the minimum and maximum line voltage as

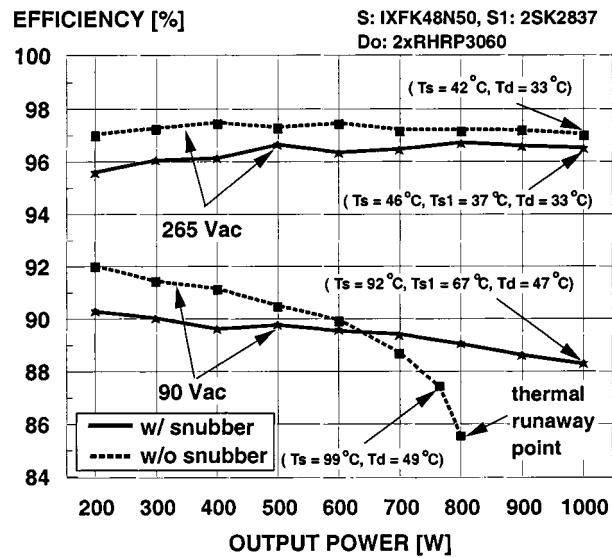


Fig. 9. Measured efficiency of 1-kW experimental circuit implemented with MOSFET boost switch.

functions of the output power. As can be seen from Fig. 8, at the high line (265 V_{ac}), the efficiency of the converter with the active snubber is slightly lower than the efficiency of the implementation without the snubber. In fact, at the high line the loss of the added active snubber circuit is larger than the reduction of the reverse-recovery-related losses of the converter without the snubber because at the high line the rectifier current and, therefore, reverse-recovery losses are relatively small. Also, at the low line (90 V_{ac}), the efficiency of the circuit with and without snubber is almost the same up to the 700-W level. However, for power levels higher than 700 W, where reverse-recovery losses are substantially increased, the active-snubber improves the efficiency significantly. In fact, the maximum power that can be obtained from the circuit without the snubber is limited to around 900 W due to the thermal runaway of the boost diode caused by excessive reverse-recovery losses. With the snubber, the circuit can deliver the full power of 1 kW with the temperature of the semiconductors well within the acceptable levels, as shown in Fig. 8.

Fig. 9 shows the measured efficiencies of the MOSFET implementation of the experimental converter with and without the active snubber at the minimum and maximum line voltages as functions of the output power. The efficiencies of the circuit with and without the snubber show a similar general trend as for the IGBT implementation, i.e., the active snubber improves the low-line efficiency at higher output power levels where the reverse-recovery losses are significant. As can be seen from Fig. 9, without the snubber, the experimental circuit could not deliver more than approximately 750 W because of the boost diode thermal runaway. With the snubber, the circuit was able to deliver the full power of 1 kW.

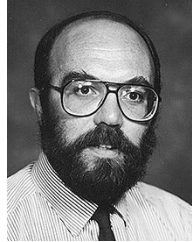
Finally, it should be noted that in the above experimental efficiency evaluations, the emphasis was on the relative efficiency comparisons between implementations with and without the snubber. No attempt was made to maximize the absolute efficiency of the experimental circuit for any implementation by selecting less lossy semiconductor or passive components.

V. CONCLUSION

A minimum-component-count active snubber which improves the performance of high-power boost converters by reducing the reverse-recovery-related losses is described. The snubber consists of a snubber inductor, rectifier, and a ground-referenced (directly) driven auxiliary switch. The voltage and current stresses of the components in the proposed active-snubber boost converter are similar to those in its conventional "hard-switched" counterpart. It was experimentally verified on a 1-kW, universal-input, boost-power-stage prototype that the proposed active snubber is effective in extending the power range of the boost converter by reducing the reverse-recovery-related losses.

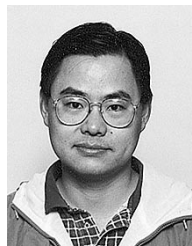
REFERENCES

- [1] Y. Khersonsky, M. Robinson, and D. Gutierrez, "New fast recovery diode technology cuts circuit losses, improves reliability," *Power Conversion Intell. Motion (PCIM) Mag.*, pp. 16–25, May 1992.
- [2] R. Streit and D. Tollik, "High efficiency telecom rectifier using a novel soft-switched boost-based input current shaper," in *Proc. Int. Telecommun. Energy Conf. (INTELEC)*, Oct. 1991, pp. 720–726.
- [3] G. Hua, C. S. Leu, and F. C. Lee, "Novel zero-voltage-transition PWM converters," in *Proc. IEEE Power Electron. Spec. Conf. (PESC) Rec.*, June 1992, pp. 55–61.
- [4] D. C. Martins, F. J. M. de Seixas, J. A. Brilhante, and I. Barbi, "A family of dc-to-dc PWM converters using a new ZVS commutation cell," in *Proc. IEEE Power Electron. Spec. Conf. (PESC) Rec.*, June 1993, pp. 524–530.
- [5] J. Bassett, "New, zero voltage switching, high frequency boost converter topology for power factor correction," in *Proc. Int. Telecommun. Energy Conf. (INTELEC)*, Oct. 1995, pp. 813–820.
- [6] M. M. Jovanović, "A technique for reducing rectifier reverse-recovery-related losses in high-voltage, high-power boost converters," in *Proc. IEEE Appl. Power Electron. (APEC) Conf.*, Mar. 1997, pp. 1000–1007.
- [7] C. M. C. Duarte and I. Barbi, "An improved family of ZVS-PWM active-clamping dc-to-dc converters," in *Proc. IEEE Power Electron. Spec. Conf. (PESC) Rec.*, May 1998, pp. 669–675.
- [8] G. Carli, "Harmonic distortion reduction schemes for a new 100A-48 V power supply," in *Proc. Int. Telecommun. Energy Conf. (INTELEC)*, 1992, pp. 524–531.
- [9] K. Smith and K. M. Smedley, "Lossless, passive soft switching methods for inverters and amplifiers," in *IEEE Power Electron. Spec. Conf. (PESC) Rec.*, 1997, pp. 1431–1439.
- [10] C. J. Tseng and C. L. Chen, "Passive lossless snubbers for dc/dc converters," in *Proc. IEEE Appl. Power Electron. Conf. (APEC)*, 1998, pp. 1049–1054.



Milan M. Jovanovic (S'86–M'89–SM'89) was born in Belgrade, Yugoslavia. He received the Dipl.-Ing. degree in electrical engineering from the University of Belgrade, Yugoslavia, the M.S.E.E. degree from the University of Novi Sad, Yugoslavia, and the Ph.D. degree in electrical engineering from the Virginia Polytechnic Institute and State University (Virginia Tech), Blacksburg.

He is the Vice President for Research and Development of Delta Products Corporation, Research Triangle Park, NC (U.S. subsidiary of Delta Electronics, Inc., Taiwan, R.O.C., one of the world's largest manufacturers of power supplies). His 23-year experience includes the analysis and design of high-frequency, high-power-density power processors; modeling, testing, evaluation, and application of high-power semiconductor devices; analysis and design of magnetic devices; and modeling, analysis, and design of analog electronics circuits. His current research is focused on power conversion and management issues for portable data-processing equipment, design optimization methods for low-voltage power supplies, distributed power systems, and power-factor-correction techniques.



Yungtaek Jang (S'92–M'95) was born in Seoul, Korea. He received the B.S. degree from Yonsei University, Seoul, Korea, in 1982, and the M.S. and Ph.D. degrees from the University of Colorado, Boulder, in 1991 and 1995, respectively, all in electrical engineering.

From 1982 to 1988, he was a Design Engineer with Hyundai Engineering Co., Seoul. From 1995 to 1996, he was a Senior Engineer with Advanced Energy Industries, Inc., Fort Collins, CO. Since 1996, he has been a Project Engineer with the Power Electronics Laboratory, Delta Products Corporation, Research Triangle Park, NC. His research interests include resonant power conversion, converter modeling, control techniques, and low harmonic rectification.